Supplementary Information

# Homogeneous Molecular Catalysis of the Electrochemical Reduction of $N_2O$ to $N_2$: Redox vs. Chemical Catalysis.

Rana Deeba,[a] Sylvie Chardon-Noblat[a,]* and Cyrille Costentin[a,b,]*

[a] Univ Grenoble Alpes, DCM, CNRS, 38000 Grenoble, France.

[b] Université de Paris, 75013 Paris, France.

*sylvie.chardon@univ-grenoble-alpes.fr*, *cyrille.costentin@univ-grenoble-alpes.fr*

## 1. Experimental Details

### Chemical

Acetonitrile (Fisher Chemical, ≥ 99.9 %, HPLC Gradient Grade), the supporting electrolyte $n$-$NBu_4PF_6$ (Sigma-Aldrich) were used as received. [Re(bpy)$(CO)_3$Cl], [Re(dmbpy)$(CO)_3$Cl] and [Mn(bpy)$(CO)_3$Br] and [Mn(dmbpy)$(CO)_3$Br] were prepared according to literature procedures. [1S,2S] All gases are supplied by Air Liquid. All organic catalysts (Table S1) are commercially available and used without further purification.

### Methods and Instrumentation

*Cyclic Voltammetry.* Cyclic voltammograms (CV) were obtained by use of CHI 750E bipostentiostat equipped with a standard three-electrode cell. The working electrode was a commercial 3 mm-diameter glassy carbon (GC) disk. Prior to the acquisition of each CV, the working electrode was polished using 2μ diamond paste (Presi) followed by rinsing with methanol. The counter electrode was a platinum wire and the reference electrode was $Ag^+/Ag$ ($AgNO_3$ 10 mM) in acetonitrile + 0.1 M $n$-$NBu_4PF_6$ in acetonitrile. The potentials are reported vs. $Ag^+/Ag$ and can be converted vs. SCE according to: $E(vs.\ \mathrm{SCE}) = E(vs.\ \mathrm{Ag^+/Ag}) + 0.28\ \mathrm{V}$ All experiments were carried out under argon or $N_2O$ at room temperature.

*Bulk electrolysis in glovebox and in situ UV-vis.* Bulk electrolysis were performed using a Biologic SP-300 potentiostat. The experiments were carried out in a glovebox in a conventional three-electrode cell with a GC plate working electrode. The reference electrode was a $Ag/Ag^+$ ($AgNO_3$ 10 mM) in acetonitrile + 0.1 M $n$-$NBu_4PF_6$ and the counter electrode a platinum wire in a bridge separated from the electrolytic cell by a glass frit, containing a 0.1M $n$-$NBu_4PF_6$ acetonitrile solution. The progress of electrolysis was followed by in situ UV-vis measurements with a Zeiss MCS501 spectrophotometer equipped with an optic fiber.

*Controlled Potential Electrolysis.* Electrolysis were performed using a Solartron Analytical Instrument potentiostat (Modulab XM MTS) using XM-studio software. The experiments were carried out in an airtight conventional three-electrode cell (25 mL) with a GC plate working electrode (1 $cm^2$), the volume of the solution was 9 mL and hence the headspace 16 mL. The reference electrode was a $Ag/Ag^+$ ($AgNO_3$ 10 mM) in acetonitrile + 0.1 M $n$-$NBu_4PF_6$ and the counter electrode a platinum wire in a bridge separated from the electrolytic cell by a glass frit, containing a 0.1M $n$-$NBu_4PF_6$ acetonitrile solution. The electrolyte solution was purged with $N_2O$ during 1h prior to electrolysis. To prevent any light induced process, the cell was covered by an aluminum foil.

*Gas detection.* Gas analysis for $N_2$ was performed using GC/MS gas chromatography (Perkin Elmer Clarus 560) instrument with column fitted with GS-QPlot column from Agilent. Temperature was held at 80 ºC for the oven. The carrier gas was Helium. Manual injections (100 µL) were performed at intervals during the experiment via a gas tight Hamilton microsyringe.

The surface of nitrogen MS (14) was integrated: $\left(A_{N_2}\right)_t$ The surface area obtained at time zero (before starting the electrolysis) is subtracted: $A_{N_2} = \left(A_{N_2}\right)_t - \left(A_{N_2}\right)_0$ . The corresponding volume of $N_2$ produced by electrolysis in the sample is obtained using a calibration curve. Then this volume was divided by the sample volume giving the percentage of nitrogen in the cell.
The calibration curve is obtained from injection of volume of $N_2$ (from 0 to 30µL).

### Calculation of the Faradaic Yield:

At a given charge passed $Q$ (in C), the % of $N_2$ in the gas phase was obtained from a peak area GC measurement from a 100 µL sample of the headspace as described above. The volume of $N_2$ in the headspace is then obtained by: $V_{N_2}(\text{mL}) = V_H \times \left(\%N_2\right)_{sample} / 100$ knowing that the volume of the headspace $V_H$. Then, considering that all the $N_2$ produced is in the gas phase, we obtained the quantity of $N_2$ produced by: $n_{N_2} = V_{N_2}(\text{mL}) / 22400(\text{mL/mol})$. Hence the faradaic yield is:

$$FY\left(N_2\right) = \frac{2n_{N_2}}{Q/F}.$$

The assumption that all the $N_2$ produced is in the gas phase is justified as follows:

The equilibrium constant for $N_{2(CH3CN)} = N_{2(g)}$ is: $K = 310^3 = \frac{P_{N_2}/P^0}{x_{N_2}}$ [3S] with $P^0 = 1$ bar. Considering $P_{N_2} = 1$ bar, the molar fraction of $N_2$ in acetonitrile is: $x_{N_2} = 3.3 \times 10^{-4}$ thus leading to a concentration of 6.4 µM making the amount of $N_2$ in solution negligible compared to the amount in the headspace in our experiments.

## 2. Organic molecular catalysts

Table S1.

| catalyst | structure |
|---|---|
| Terephthalonitrile<br>(1,4-dicyanobenzene) | 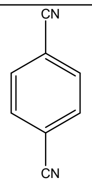 |
| Phthalonitrile<br>(1,2-dicyanobenzene) | 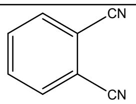 |
| perylene | 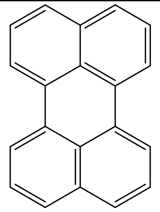 |
| Benzophenone<br>(diphenylmethanone) | 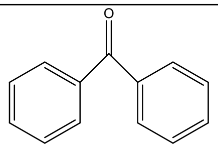 |
| 4-cyanopyridine | 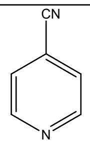 |
| 1-naphthonitrile<br>(1-cyanonaphthalene) | 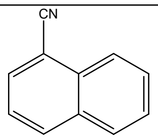 |
| 9,10-diphenylanthracene | 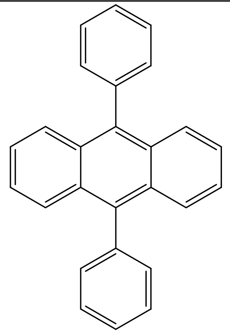 |
| anthracene | 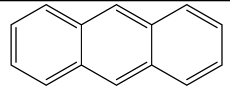 |

| | |
|---|---|
| 9,10-dimethylanthracene | 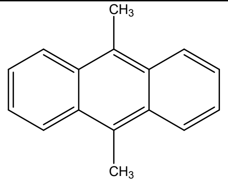 |
| fluorenone | 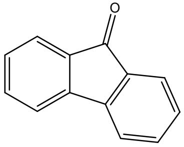 |
| 9,10-dicyanoanthracene | 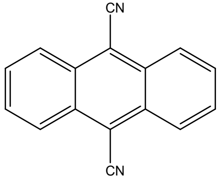 |
| Phenazine<br>(9,10-diazaanthracene) | 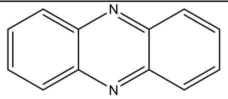 |

## 3. Controlled potential electrolysis

.

Short-time electrolysis were performed at a controlled potential under $N_2O$ in acetonitrile with $n$-$Bu_4NPF_6$ (0.1 M) and 100 mM of $H_2O$ on a 1 $cm^2$ carbon electrode. When present, the catalyst concentration is 1 mM. Results are gathered in Table S2 and figure S1.

Table S2. $N_2O$ reduction electrolysis

| Catalyst | Applied Potential (V vs. $Ag^+/Ag$) | Charge passed (C) | $V_{N2}$ (mL) | Faradaic yield [a] |
|---|---|---|---|---|
| phthalonitrile | -2.15 | 2.45 | 0.21 | 74 |
| benzophenone | -2.15 | 17 | 2.31 | 117 |
| perylene | -2.15 | 17.47 | 2.05 | 101 |
| 4-cyanopyridine | -2.15 | 3.0 | 0.38 | 109 |
| [Re(bpy)$(CO)_3$Cl] | -2.2 | 7.16 | 0.98 | 118 |
| No catalyst | -2.45 | 4.22 | 0.60 | 123 |

[a] based on a stoichiometry equal to 2

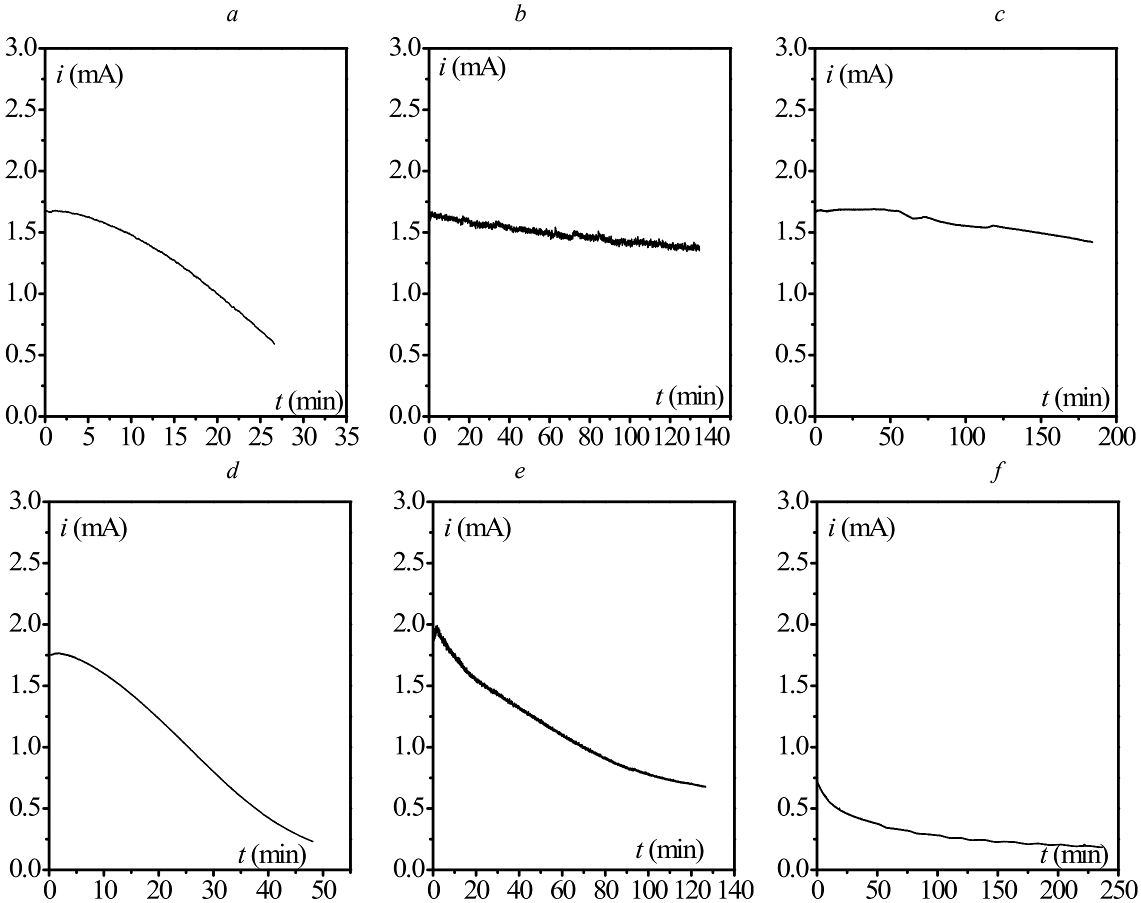

Fig. S1. Current vs. time for controlled potential electrolysis in the conditions given in Table S2 and above. (a) Phthalonitrile (b) Benzophenone (c) Perylene (d) 4-cyanopyridine (e) [Re(bpy)$(CO)_3$Cl] (e) No catalyst.

## 4. Additional CVs

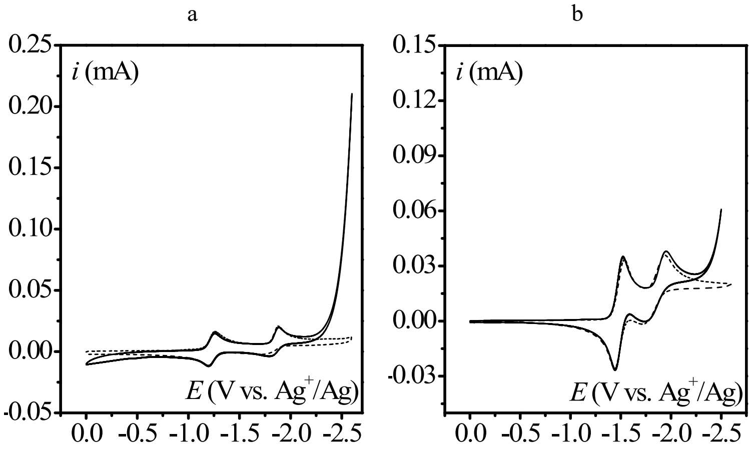

Fig. S2. CVs of the catalyst (under argon at 0.1 V/s (dashed line) and under $N_2O$ (full line) in acetonitrile with *n*-$Bu_4NPF_6$ (0.1 M) on a 3 mm diameter glassy carbon electrode at 0.1 V/s. (a) dicyanoanthracene (0.5 mM) (b) phenazine (1 mM).

## 5. Effect of scan rate

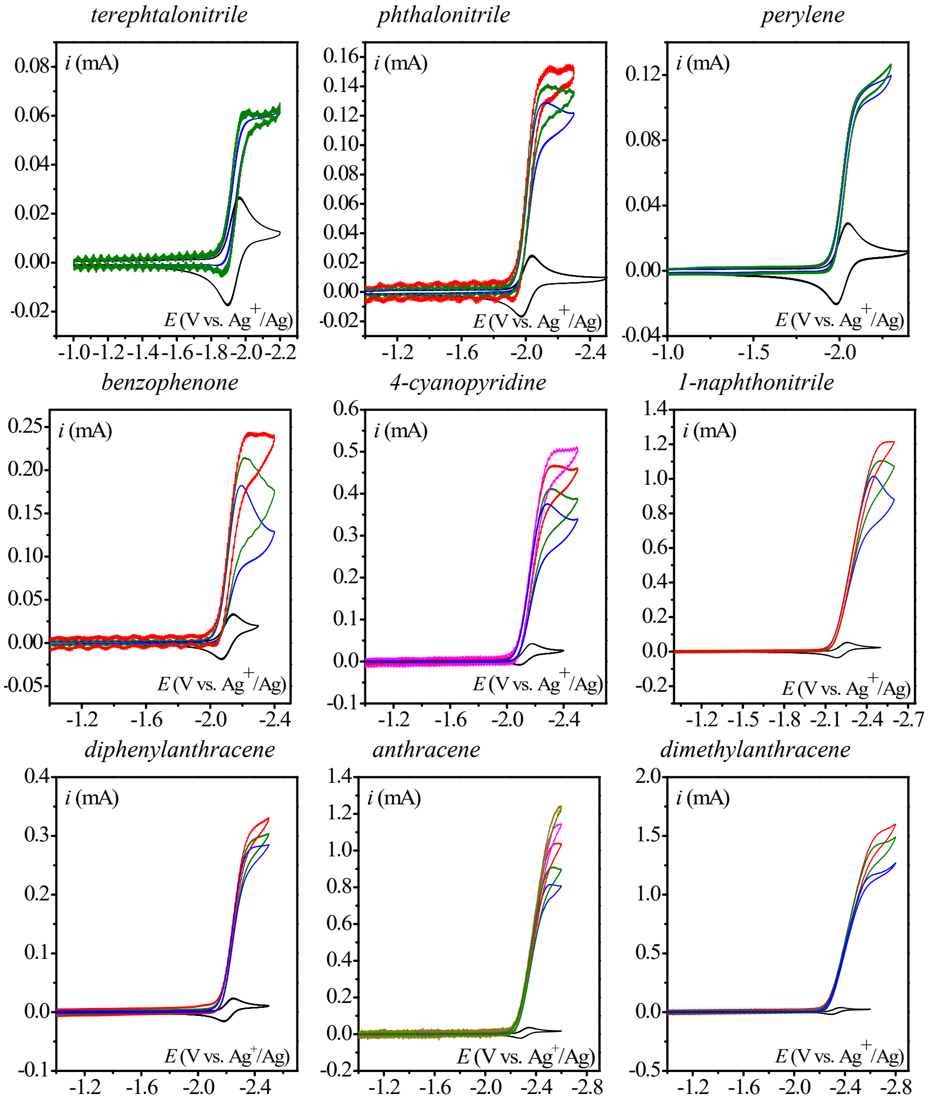

*terephtalonitrile* *phthalonitrile* *perylene*

*benzophenone* *4-cyanopyridine* *1-naphthonitrile*

*diphenylanthracene* *anthracene* *dimethylanthracene*

Fig. S3. Homogeneous catalysis of the electrochemical reduction of $N_2O$ by organic radical anions. CVs of the catalyst (1 mM) under argon at 0.1 V/s (black) and under $N_2O$, in acetonitrile with *n*-$Bu_4NPF_6$ (0.1 M) on a 3 mm diameter glassy carbon electrode. **Terephthalonitrile** v = 0.1 (blue), 0.2 (green)V/s. **Phthalonitrile** v = 0.1 (blue), 0.2 (green), 0.5 (red). **Perylene** v = 0.1 (blue), 0.2 (green) V/s. **Benzophenone** v = 0.1 (blue), 0.2 (green), 0.5 (red) V/s. **4-cyanopyridine** v = 0.1 (blue), 0.2 (green), 0.5 (red), 1 (magenta) V/s. **1-naphthonitrile** v = 0.1 (blue), 0.2 (green), 0.5 (red) V/s. **9,10-diphenylanthrace**ne v = 0.1 (blue), 0.2 (green), 0.5 (red) V/s. **Anthracene** v = 0.1 (blue), 0.2 (green), 0.5 (red), 1 (magenta), 2 (dark yellow) V/s. **9,10-dimethylanthracene** v = 0.2 (blue), 1 (green), 2 (red) V/s.

### 6. Ohmic drop correction

The resistance between the working electron and the reference electrode is evaluated using the manual positive feedback compensation of the potentiostat. The positive feedback was manually increased until sustained oscillations are observed upon scanning in a range of potential where there is only capacitive current.$^{,4S}$ The obtained value is $R_u$ = 120 ohms. A correction of $R_\mathrm{u}$ x $i$ was applied on the potential axis f the raw data (figure S3).

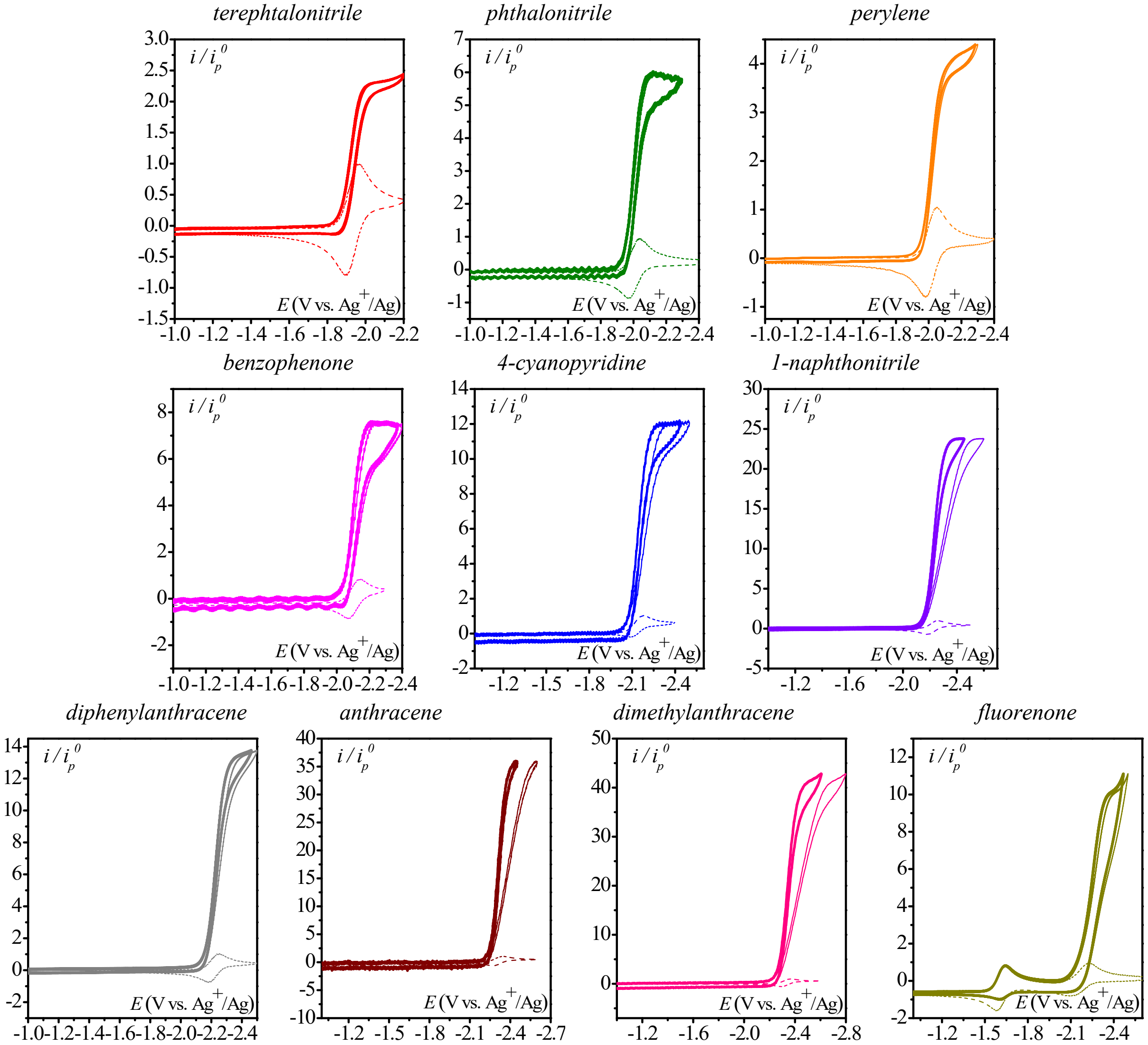

Fig. S4. Homogeneous catalysis of the electrochemical reduction of $N_2O$ by radical anions or dianion. Normalized CVs of the catalyst (1 mM) under argon at 0.1 V/s (dashed line) and under $N_2O$ (full line) and after ohmic drop correction (thick line) at a scan rate allowing to reach the catalytic plateau current, in acetonitrile with $n$-$Bu_4NPF_6$ (0.1 M) on a 3 mm diameter glassy carbon electrode. $i_p^0 = 0.446 FSC_\mathrm{cat}^0 \sqrt{DFv/RT}$ . $S$ is the electrode surface area, $C_\mathrm{cat}^0$ is the catalyst concentration, $D$ the catalyst diffusion coefficient, $F$ the Faraday, $R$ the gas constant, $T$ the temperature. **Terephthalonitrile** v = 0.1 V/s. **Phthalonitrile** v = 0.2 V/s. **Perylene** v = 0.1 V/s. **Benzophenone** v = 0.5 V/s. **4-cyanopyridine** v = 1 V/s. **1-naphthonitrile** v = 0.5 V/s. **9,10-diphenylanthracen**e v = 0.2 V/s. **Anthracene** v = 2 V/s. **9,10-dimethylanthracene** v = 2 V/s. **Fluorenone** v = 0.1 V/s.

## 7. Kinetic analysis

We consider the reaction scheme S1 in the framework of cyclic voltammetry with excess of substrate ($N_2O$) and cosubstrate ($H_2O$) and pure kinetics conditions (fast catalysis). The homogenous second step (homogeneous electron transfer) is assumed to be fast so that the intermediate is at steady-state.. The heterogeneous electron transfer is characterized by a standard potential $E^0_{cat}$ and assumed to be fast (nernstian).

**Scheme S1.**

$$\mathrm{P} + \mathrm{e} \rightleftharpoons \mathrm{Q}$$

$$\mathrm{Q} + \mathrm{N_2O} \xrightarrow{k} \text{intermediate}$$

$$\mathrm{Q} + \text{intermediate} \xrightarrow{\text{fast}} \mathrm{N_2} + \text{co-products} + 2\,\mathrm{P}$$

At $t = 0$ and $\forall x$ ($x$ is the distance from the electrode surface) and at $x = \infty$ and $\forall t$, $C_{\mathrm{P}} = C^0_{\mathrm{cat}}$ and $C_{\mathrm{Q}} = 0$

Governing equations:

$$\frac{\partial C_{\mathrm{P}}}{\partial t} = D\frac{\partial^2 C_{\mathrm{P}}}{\partial x^2} + 2k_e C_{\mathrm{Q}} C_{\mathrm{I}}$$

$$\frac{\partial C_{\mathrm{Q}}}{\partial t} = D\frac{\partial^2 C_{\mathrm{Q}}}{\partial x^2} - kC_{\mathrm{Q}}C_{\mathrm{N_2O}} - k_e C_{\mathrm{Q}} C_{\mathrm{I}}$$

$$\frac{\partial C_{\mathrm{I}}}{\partial t} = D\frac{\partial^2 C_{\mathrm{I}}}{\partial x^2} + kC_{\mathrm{Q}}C_{\mathrm{N_2O}} - k_e C_{\mathrm{Q}} C_{\mathrm{I}}$$

All species are assumed to have the same diffusion coefficient $D$.

Additional boundary condition at $x = 0$ and $t > 0$

$$\left[\frac{\partial C_{\mathrm{Q}}}{\partial x}\right]_{x=0} = -\left[\frac{\partial C_{\mathrm{P}}}{\partial x}\right]_{x=0} = -\frac{i}{FSD};$$

$$\left(C_{\mathrm{P}}\right)_{x=0} = \left(C_{\mathrm{Q}}\right)_{x=0} \exp\left[\frac{F\left(E - E^0_{cat}\right)}{RT}\right]$$

Resolution:

*Pure kinetics conditions:*

$$D\frac{\partial^2 C_{\mathrm{Q}}}{\partial x^2} = kC_{\mathrm{Q}}C_{\mathrm{N_2O}} + k_e C_{\mathrm{Q}} C_{\mathrm{I}}$$

*Steady-state on Q':*

$kC_{\mathrm{Q}}C_{\mathrm{N_2O}} + k_e C_{\mathrm{Q}} C_{\mathrm{I}}$ leading to

$$D\frac{\partial^2 C_{\mathrm{Q}}}{\partial x^2} = 2kC_{\mathrm{Q}}C_{\mathrm{N_2O}}$$

Resolution of $D\frac{\partial^2 C_{\mathrm{Q}}}{\partial x^2} = 2kC_{\mathrm{Q}}C_{\mathrm{N_2O}}$ taking into account boundary conditions leads to:

$$\left(C_{\mathrm{Q}}\right)_{x=0} = \frac{i}{FS\sqrt{D}\sqrt{2kC_{\mathrm{N_2O}}}} = \frac{i}{FS\sqrt{D}\sqrt{2k_{cat}}}.$$

Moreover, we have:

$$\frac{\partial\left(C_{\mathrm{P}}+C_{\mathrm{Q}}+C_{\mathrm{I}}\right)}{\partial t} = D\frac{\partial^2\left(C_{\mathrm{P}}+C_{\mathrm{Q}}+C_{\mathrm{I}}\right)}{\partial x^2}$$ which integration taking into account boundary conditions leads to:

$$C_{cat}^0 = \left(C_{\mathrm{P}}+C_{\mathrm{Q}}+C_{\mathrm{I}}\right)_{x=0} \approx \left(C_{\mathrm{P}}+C_{\mathrm{Q}}\right)_{x=0}$$

We finally obtain, taking into account $i_p^0 = 0.446FSC_{\mathrm{cat}}^0\sqrt{DFv/RT}$ :

$$\frac{i_{pl}}{i_p^0} = 2.24\sqrt{\frac{RT}{Fv}}\sqrt{2k}$$

and

$$\frac{i}{i_p^0} = \frac{i_{pl}/i_p^0}{1+\exp\left[\frac{F}{RT}\left(E-E_{cat}^0\right)\right]} \qquad \text{(S1)}$$

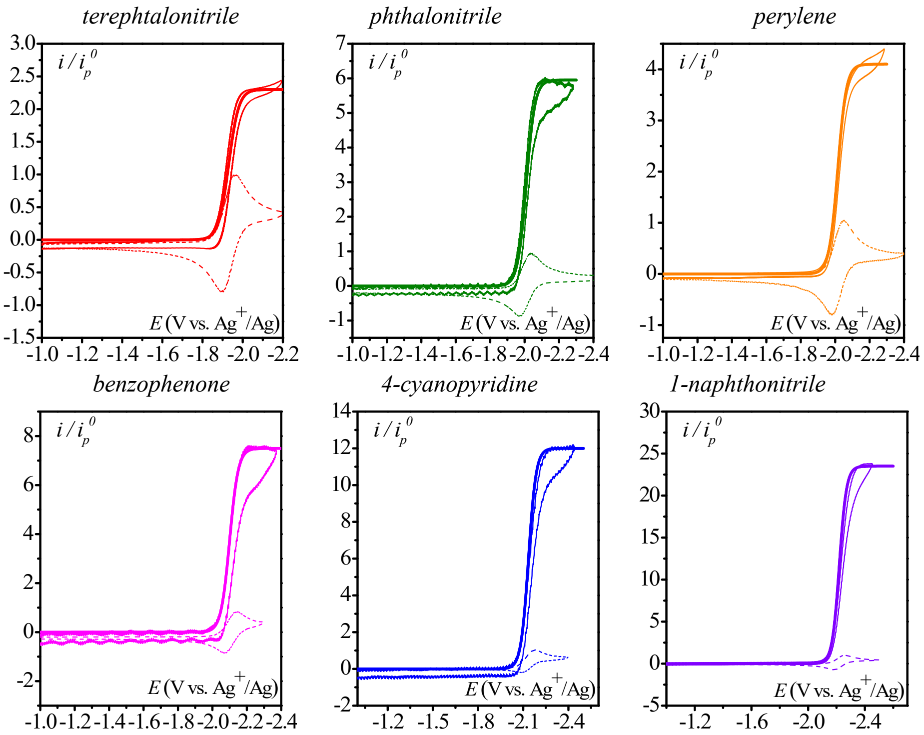

*diphenylanthracene* *anthracene* *dimethylanthracene* *fluorenone*

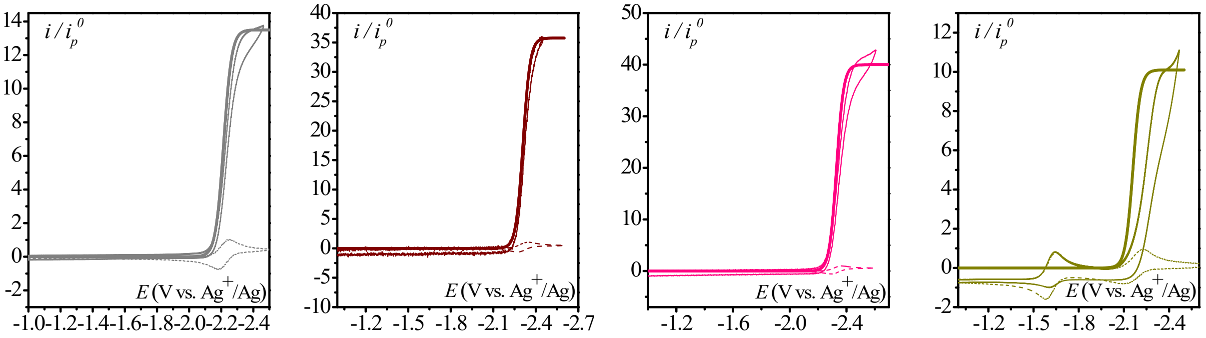

Fig. S5. Homogeneous catalysis of the electrochemical reduction of $N_2O$ by radical anions or dianion. Normalized CVs of the catalyst (1 mM) under argon at 0.1 V/s (dashed line) and under $N_2O$ (full line) (after ohmic drop correction) at a scan rate allowing to reach the catalytic plateau current, in acetonitrile with *n*-$Bu_4NPF_6$ (0.1 M) on a 3 mm diameter glassy carbon electrode. $i_p^0 = 0.446FSC_{\mathrm{cat}}^0\sqrt{DFv/RT}$ . $S$ is the electrode surface area, $C_{\mathrm{cat}}^0$ is the catalyst concentration, $D$ the catalyst diffusion coefficient, $F$ the Faraday, $R$ the gas constant, $T$ the temperature. **Terephthalonitrile** v = 0.1 V/s. **Phthalonitrile** v = 0.2 V/s. (c) **Perylene** v = 0.1 V/s. **Benzophenone** v = 0.5 V/s. **4-cyanopyridine** v = 1 V/s. **1-naphthonitrile** v = 0.5 V/s **9,10-diphenylanthracene** v = 0.2 V/s. **Anthracene** v =2 V/s. **9,10-dimethylanthracene** v = 2 V/s. **Fluorenone** v = 0.1 V/s. Thick lines: fitting with equation (S1).

## 8. Direct reduction: effect of scan rate

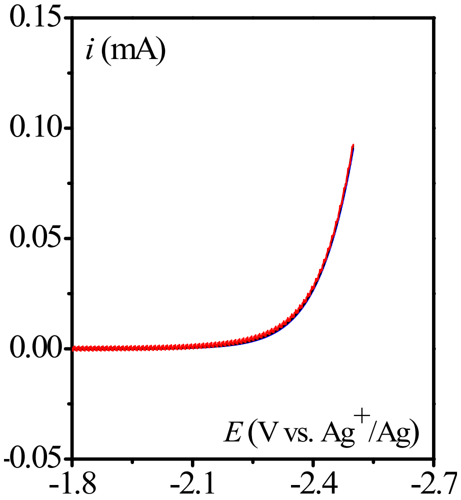

Fig S6. Linear scan voltammetry of direct reduction of $N_2O$ in acetonitrile with *n*-$Bu_4NPF_6$ (0.1 M) on a 3 mm diameter glassy carbon electrode. $v$ = 0.1 (blue), 0.2 (black), 0.5 (red) V/s. Current is offset at zero at -1.8 V to subtract the scan rate dependent capacitive contribution.

## 9. Standard potentials of $[\mathrm{Re^{I}(L^{\bullet-})(CO)_3}]/[\mathrm{Re^{0}(L^{\bullet-})(CO)_3}]^-$ couples.

Bulk electrolysis of a $[\mathrm{Re(L)(CO)_3Cl}]$ 1 mM solution was performed in a glovebox on a glassy carbon plate electrode. Two equivalents of electrons are passed to form the anion $[\mathrm{Re^{0}(L^{\bullet-})(CO)_3}]^-$. Formation of $[\mathrm{Re^{0}(L^{\bullet-})(CO)_3}]^-$ was assessed by recording a situ UV-vis spectrum (figures S7 a and b) and comparison with previously reported data.[,5S] A CV was then recorded on a 3 mm diameter glassy carbon electrode at 0.1 V/s (figures S7 c and d) showing a partially reversible one electron wave corresponding to the $[\mathrm{Re^{I}(L^{\bullet-})(CO)_3}]/[\mathrm{Re^{0}(L^{\bullet-})(CO)_3}]^-$ couples. The standard potential was evaluated from mid-point potential between the anodic and cathodic peak potentials.

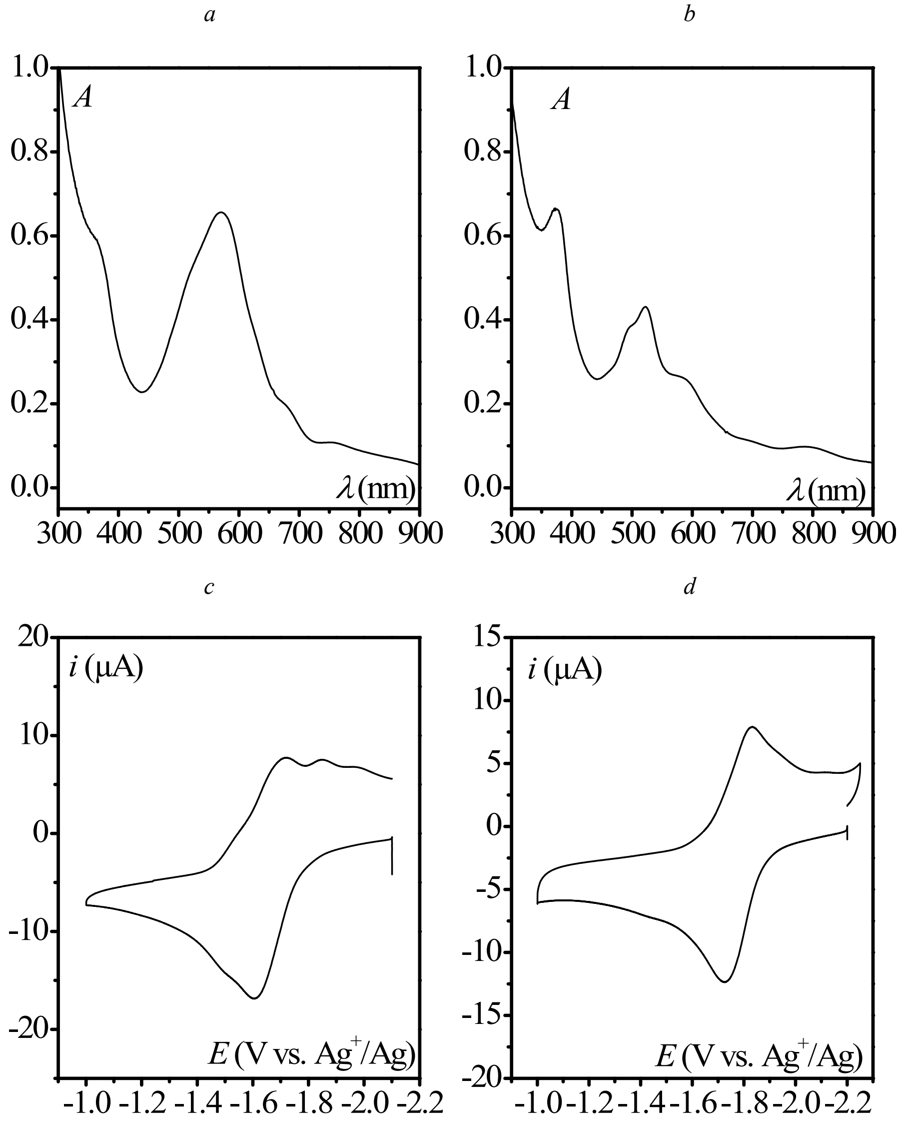

Fig S7. (a, b) UV-vis spectrum and (c, d) CV at 0.1 V/s on a 3 mm diameter glassy carbon electron of electrogenerated $[\mathrm{Re(L)(CO)_3}]^-$ (a,c: L =bpy; b,d: L=dmbpy) in $\mathrm{CH_3CN}$ + 0.1 M $\mathrm{NBu_4PF_6}$ under inert atmosphere (glovebox).

## 10. References:

1S. (a) Sullivan, B. P.; Bolinger, C. M; Conrad, D.; Vining, W. J.; Meyer, T. J. One- and Two-electron Pathways in the Electrocatalytic Reduction of $CO_2$ by *fac*-Re(bpy)$(CO)_3$Cl (bpy = 2,2'-bipyridine) *J. Chem. Soc., Chem. Commun.* **1985**, 1414-1416. (b) Stor, G. J.; Hartl, F.; van Outerstep, J. W. M.; Stufkens, D. J. Spectroelectrochemical (IR, UV/Vis) Determination of the Reduction Pathways for a Series of $[Re(CO)_3(\alpha\text{-diimine})L']^{0/+}$ (L' = Halide, $Otf^-$, THF, MeCN, *n*-PrCN, $PPh_3$, $P(OMe)_3$) Complexes. *Organometallics* **1995**, *14*, 1115-1131. (c) Machan, C. W.; Sampson, M. D.; Chabolla, S. A.; Dang, T.; Kubiak, C. P. Developing a Mechanistic Understanding of Molecular Electrocatalysts for $CO_2$ Reduction using Infrared Spectroelectrochemistry. *Organometallics* **2014**, *33*, 4550-4559.

2S. Bourrez, M.; Molton, F.; Chardon-Noblat, S.; Deronzier, A. $[Mn(bipyridyl)(CO)_3Br]$ : An Abundant Metal Carbonyl Complex as Efficient Electrocatalyst for $CO_2$ Reduction. *Angew. Chem. Int. Ed.* **2011**, *50*, 9903-9906.

3S. Battino, R.; Rettich, T. R.; Tominaga, T. The Solubility of Nitrogen and Air in Liquids. *J. Phys. Chem. Ref. Data* **1984**, *13*, 563-600.

4S. Costentin, C.; Savéant, J.-M. Elements of Molecular and Biomolecular Electrochemistry, 2nd Ed., Wiley, 2019, pp 10-18.

5S. (a) For $[Re(bpy)(CO)_3]^-$, see: Fujita, E.; Muckerman, J. T. Why is Re-Re Bond Formation/Cleavage in $[Re(bpy)(CO)_3]_2$ Different from That in $[Re(CO)_5]$? Experimental and Theoretical Studies on the Dimers and Fragments. *Inorg. Chem*. **2004**, *4*3, 7636-7647. (b) For $[Re(dmbpy)(CO)_3]^-$, see: Cosnier, S. PhD dissertation, Université Joseph Fournier (Grenoble I), France, 1988.